Journal of Atmospheric and Solar-Terrestrial Physics 138-139 (2016) 112–120

Contents lists available at ScienceDirect

Journal of Atmospheric and Solar-Terrestrial Physics

journal homepage: www.elsevier.com/locate/jastp

Latin American Lidar Network (LALINET) for aerosol research: Diagnosis on network instrumentation

Juan Luis Guerrero-Rascado [a,b,c,*], Eduardo Landulfo [a], Juan Carlos Antuña [d], Henrique de Melo Jorge Barbosa [e], Boris Barja [d,e], Álvaro Efrain Bastidas [f], Andrés Esteban Bedoya [f], Renata Facundes da Costa [a], René Estevan [d], Ricardo Forno [g], Diego Alvés Gouveia [e], Cristofer Jiménez [h,i], Eliane Gonçalves Larroza [a], Fábio Juliano da Silva Lopes [a,j], Elena Montilla-Rosero [h,i], Gregori de Arruda Moreira [a], Walker Morinobu Nakaema [a], Daniel Nisperuza [f], Dairo Alegria [f], Mauricio Múnera [f], Lidia Otero [k], Sebastián Papandrea [k], Juan Vicente Pallota [k], Ezequiel Pawelko [k], Eduardo Jaime Quel [k], Pablo Ristori [k], Patricia Ferrini Rodrigues [a], Jacobo Salvador [k], Maria Fernanda Sánchez [g], Antonieta Silva [h,l]

[a] Centro de Lasers e Aplicações, Instituto de Pesquisas Energéticas e Nucleares (IPEN), Avd. Prof. Lineu Prestes 2242, 05508-000 São Paulo, Brazil
[b] Instituto Interuniversitario de Investigación del Sistema Tierra en Andalucía (IISTA-CEAMA), Av. del Mediterráneo, 18006 Granada, Spain
[c] Universidad de Granada, Dpto. Física Aplicada, Fuentenueva s/n, 18071 Granada, Spain
[d] Centro Meteorológico de Camagüey, Instituto de Meteorología de Cuba, 70100, Cuba
[e] Instituto de Física, Universidade de São Paulo, Rua do Matão, Travessa R, 187, 05508-090 São Paulo, Brazil
[f] Escuela de Física, Universidad Nacional de Colombia, Calle 59ª N° 63-20, 050034 Medellín, Colombia
[g] Laboratorio de Física de la Atmósfera, Universidad Mayor de San Andrés, Casilla 8635, La Paz, Bolivia
[h] Centro de Óptica y Fotónica CEFOP, Universidad de Concepción, Casilla 4016, Concepción, Chile
[i] Universidad de Concepción, Dpto. Física, Casilla 160-C, Concepción, Chile
[j] Universidade de São Paulo, Instituto de Astronomia, Geofísica e Ciências Atmosféricas, Rua do Matão, 1226, Cidade Universitária, 05508-000 São Paulo, Brazil
[k] División Lidar, CEILAP (UNIDEF-CONICET), San Juan Bautista de La Salle 4397, B1603ALO, Villa Martelli, Buenos Aires, Argentina
[l] Dpto. Ciencias Físicas, Universidad de La Frontera, Casilla 54-D, Temuco, Chile

ARTICLE INFO

Article history:
Received 21 September 2015
Received in revised form
30 December 2015
Accepted 4 January 2016
Available online 6 January 2016

Keywords:
Aerosol detection
Lidar
Networks
Remote sensing and sensors

ABSTRACT

LALINET (Latin American Lidar Network), previously known as ALINE, is the first fully operative lidar network for aerosol research in South America, probing the atmosphere on regular basis since September 2013. The general purpose of this network is to attempt to fill the gap in the knowledge on aerosol vertical distribution over South America and its direct and indirect impact on weather and climate by the establishment of a vertically-resolved dataset of aerosol properties. Similarly to other lidar research networks, most of the LALINET instruments are not commercially produced and, consequently, configurations, capabilities and derived-products can be remarkably different among stations. It is a fact that such un-biased 4D dataset calls for a strict standardization from the instrumental and data processing point of view. This study has been envisaged to investigate the ongoing network configurations with the aim of highlighting the instrumental strengths and weaknesses of LALINET.

1. Introduction

It is well known that a detailed characterization of atmospheric aerosol particles is indispensable to thoroughly understand their role in a wide range of atmospheric processes, which impacts from climate to human health. Nonetheless, according to the Fifth Assessment Report of the Intergovernmental Panel on Change Climate (5th IPCC), atmospheric aerosol particles are still considered one of the major uncertainties in climate forcing due to their extreme variability in space and time (Boucher et al., 2013). For instance, a recent study reported a 34-year, multi-regional analysis of aerosol load showing that aerosol optical depth (AOD) prior to the 90s was relatively constant in most regions analyzed, but after that decade a positive AOD trend was found over several regions of

* Corresponding author at: Universidad de Granada, Dpto. Física Aplicada, Fuentenueva s/n, 18071 Granada, Spain
E-mail address: rascado@ugr.es (J.L. Guerrero-Rascado).

http://dx.doi.org/10.1016/j.jastp.2016.01.001
1364-6826/

the planet, including South America (Wang et al., 2009; Hartmann et al., 2013).

Although the global aerosol particles field should be continuously monitored on global scale, the available infrastructure in South America is still limited to a certain extent. For instance, there are only 30 AERONET (Aerosol Robotic Network) (Holben et al., 1998) stations in 2015 over a South American area of $18 \cdot 10^6$ km^2 (compare with 25 stations over Spain and Portugal with an area 30 times lower), thus posing a challenge to perform long-term aerosol monitoring. Furthermore, routine information on particle vertical distribution over whole South America is almost missing. Therefore most studies willing to investigate the vertical aerosol distribution in the region relied on short field campaigns. As an example, a 3-month campaign of lidar measurements was coordinated with sun-photometer and air quality data providing a better understanding of the relationship between aerosol optical properties and direct air quality measurements at the megacity of São Paulo (Brazil) (Landulfo et al., 2010). During the field campaigns of the CHUVA project (Machado et al., 2014), a portable Raman lidar was used to provide cloud and aerosol extinction profiles and cloud thickness to contribute to the understanding of cloud processes, which represent one of the least understood components of the climate system. At Concepción (Chile) lidar measurements were used to characterize the vertical distribution of aerosols revealing the potential of this technique to pollution studies in the region (Silva, 2012). More statistically relevant research was conducted with a 1-year analysis of systematic multiwavelength polarization Raman lidar observations of aerosol optical and microphysical properties over the Amazon Basin in 2008 (Baars et al., 2012). One could argue that satellite-based instrumentation could provide the missing observations of the aerosols vertical distribution in the region, but their typical small swath and large interval between overpasses limit its application to continuously monitoring climate-relevant aerosol particles such as those generated in volcano eruptions, long-range transported from Sahara desert and biomass burning from the African savanna. Therefore, the local and global scientific communities could, indeed, profit from the establishment of a ground-based network of lidar stations providing homogenized and quality-assured measurements.

LALINET (http://lalinet.org) started on voluntary basis in 2001. In March 2013 LALINET signed an agreement with the World Meteorological Organization (WMO) with the purpose of recognizing the LALINET observational network as a contributing network to the Global Atmosphere Watch (GAW) programme of the WMO, in particular to GALION (GAW Aerosol Lidar Observation Network). The main goal of LALINET is to provide a comprehensive, quantitative, and statistically significant database for the

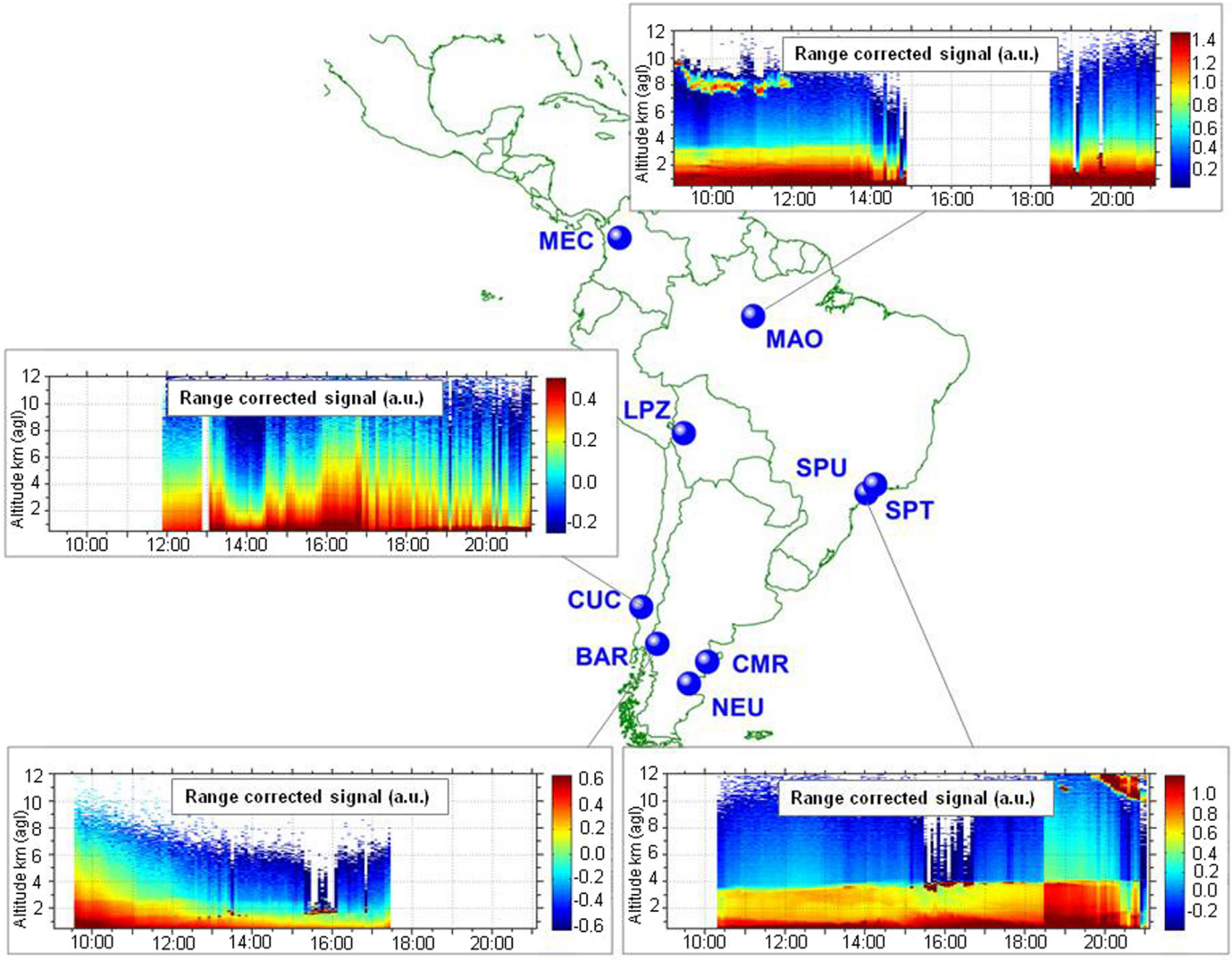

Fig. 1. LALINET Lidar stations with an example of network measurements performed on 12th September 2012 during a pilot field campaign.

vertical aerosol particle distribution over South America. This network focuses on monitoring vertical profiles of particle optical properties, i.e. particle backscatter and extinction profiles, but their microphysical properties and profiling of other atmospheric components such as water vapor, ozone and clouds are also considered. The network routinely runs measurements scheduled every Monday and Thursday from 12:00 to 15:00 and 21:00 to 00:00 UTC. LALINET currently consists of 7 groups operating 9 stations distributed over South America, covering the domain 46°S to 6°N (from Argentina to Colombia) and 47–73°W (from Brazil to Chile) (Fig. 1). Fig. 1 also shows an example of the lidar measurements (time series of 1-min range corrected signals at 532 nm) acquired during a pilot field campaign, which took place simultaneously at different LALINET sites from 10 to 14 September 2012 (Barbosa et al., 2014). Even though LALINET is currently a well-established network, most of its systems are not commercially produced and consequently configurations, capabilities and derived-products can be remarkably different between stations. It was soon recognized the utmost importance of setting quality assurance standards for both the instruments and data processing routines. Since then, three different working groups have been launched to address this commitment (Antuña et al., submitted for publication). In particular, the present study has been envisaged to investigate the ongoing network configurations with the aim of highlighting the instrumental strengths and weaknesses of LALINET.

2. Methodology

A technical specification inventory was designed to collect the instrumental features of the rather inhomogeneous LALINET systems. The information for each instrument was organized in different blocks, whose main features are listed as follows:

- Station information: official name, location, geographical coordinates, starting year of operation and environment type.
- Operation mode: zenith-pointing/scanning capabilities, automatic operation, transportability.
- Emitter subsystem: laser model, wavelengths, energy per pulse, polarization, beam diameter and divergence both before/after expansion.
- Receiver subsystem: telescope type, primary/secondary mirrors diameter, focal length, field of view and telescope-laser axes distance.
- Detection subsystem: elastic/Raman wavelengths detected, day/night capabilities, full width at half maximum of filters, detector types.
- Acquisition subsystem: detection mode, vertical and temporal resolutions, maximum range probed.
- Ancillary instrumentation: availability of permanent instrumentation close to the LALINET station.

3. Results and discussion

3.1. Station information and operation mode

Table 1 lists the LALINET lidar systems with their official station names used in GAWSIS (station information system) of GAW, locations, geographical coordinates, starting year of operation and environment type. The Camagüey station, not included in Table 1 and Fig. 1, was only operative in the period 1992–1998 and it is expected to be operative again in a few years (Antuña et al., 2012).

Currently measurements in all LALINET stations are scheduled on Mondays and Thursdays at 12:00–15:00 UTC and 21:00–00:00 UTC. Table 2 lists the main features related to the mode of operation. Most of the capabilities in a lidar system are constrained by its pointing design. Thus, traditional zenith-pointing lidar are able to retrieve particle optical properties such as the particle backscatter coefficient, particle extinction coefficient, particle lidar ratio, particle depolarization ratio (Fernald et al., 1972; Fernald, 1984; Klett, 1981, 1985; Ansmann et al., 1992; Cairo et al., 1999; Freudenthaler et al., 2009) in the vertical coordinate and analogous properties for water clouds (Hu et al., 2006). Seven of the LALINET systems (around 77.8%) are zenith-pointing lidar. Furthermore, off-zenith lidars are able to additionally determine particle and cloud optical properties in other directions (therefore increasing their capabilities to assess homogeneity in the particle/cloud field) and also different atmospheric targets located in specific directions. In particular, lidars offering full scanning capabilities are operated for particles and water/ice clouds research and for investigating properties of industrial flare stacks (da Costa et al., 2011, 2013; Guerrero-Rascado et al., 2014). Lidars configured a few degrees off the zenithal direction are devoted to ice cloud research. This is necessary to avoid specular reflections on horizontally-oriented plate-like ice crystals, which would otherwise lead to unexpected low depolarization ratios, and hence to erroneous determination of cloud backscatter coefficients (Noel and Sassen, 2004; Takano and Jayaweera, 1985; Thomas et al., 1990; Platt, 1978; Sassen, 1991). Therefore, the system MAO in the core of Amazon region, regularly operating at 5° off-zenith, is currently the only station qualified to properly monitor cirrus clouds in LALINET, even without depolarization capabilities at present (Barbosa et al., 2014). Fig. 2 illustrates clouds measurements acquired by this system from 18:00 UTC on 2nd June to 15:00 UTC on 3rd June 2014. The time serie of lidar range corrected signal at 355 nm shows the presence of an aerosol layer of relatively constant vertical extent with some capping low clouds in the first evening and in the morning of the next day. Nighttime was characterized by the presence of cirrus clouds extending from 12 to 16 km agl. Cirrus cloud optical depths (COD), derived by the transmittance method (Gouveia et al., 2014), based on the comparison of lidar range corrected signals at the base and top of the clouds, were mostly below 0.20; however values as high as 0.57 were measured.

Table 1
List of lidar systems part of LALINET and information regarding the stations. Systems marked with asterisk have a transient ID.

Lidar system (GAW ID)	City/country	Coordinates and elevation asl	Starting year	Environment type
BAR*	Bariloche/Argentina	41.15°S 71.16°W 840 m	2002	Urban/suburban
CMR	Comodoro Rivadavia/Argentina	45.78°S 67.50°W 46 m	Oct 2012	Urban/suburban
CUC	Concepción/Chile	36.84°S 73.03°W 170 m	Feb 2012	Urban
LPZ	La Paz/Bolivia	16.52°S 68.03°W 3420 m	Jun 2010	Urban
MAO	Manaus/Brazil	2.60°S 60.21°W 450 m	Feb 2011	Forest with some land use impact around
MEC	Medellin/Colombia	6.26°N 75.58°W 1463 m	Dec 2012	Urban
NEU*	Neuquén/Argentina	38.95°S 68.14°W 271 m	Dec 2013	Urban/suburban
SPT*	São Paulo/Brazil	23.56°S 46.74°W 760 m	Apr 2009	Urban
SPU	São Paulo/Brazil	23.56°S 46.74°W 760 m	Dec 2001	Urban

Table 2
Some technical specifications regarding the mode of operation for the LALINET lidar stations.

Lidar system	Pointing	Unattended operation	Mobile system
BAR	Zenith	No	Yes
CMR	Zenith	No	Yes
CUC	Zenith	No	No
LPZ	Scanning	No	Yes
MAO	5°off-zenith	Yes	Yes
MEC	Zenith	No	No
NEU	Zenith	No	Yes
SPT	Zenith	No	Yes
SPU	Zenith	No	No

Table 3
Some technical specifications regarding the emitter subsystem for the LALINET lidar stations.

Lidar system	Laser model	Repetition rate (Hz)	Wav. (nm)	Laser beam diam. (mm)	Beam exp. factor	Beam diverg. (mrad) (before/after exp.)
BAR	Brilliant	20	355	6	× 1	0.5/0.5
			532		× 1	0.5/0.5
			1064		× 1	0.5/0.5
CMR	Surelite I-30	30	355	6	× 1	0.5/0.5
			532		× 1	0.5/0.5
			1064		× 1	0.5/0.5
CUC	Brilliant B	10	355	9	× 5	0.5/0.1
			532		× 5	0.5/0.1
			1064		× 5	0.5/0.1
LPZ	Brio	1,2,5,10,20	355	3.3	× 5	1.9/0.4
			532		× 5	1.9/0.4
			1064		× 5	1.9/0.4
MAO	CFR400-10	10	355	5.3	× 4	0.7/0.2
MEC	Handy YAG H700	10,20,30,50	355	7	× 3	0.5/0.2
			532		× 3	0.5/0.2
			1064		× 3	0.5/0.2
NEU	Surelite I-30	30	355	6	× 1	0.5/0.5
			532		× 1	0.5/0.5
			1064		× 1	0.5/0.5
SPT	CFR200	20	532	6.4	× 3	0.4/0.13
SPU	Brilliant B	10	355	9	× 5	0.5/0.1
			532		× 5	0.5/0.1
			1064		× 5	0.5/0.1

Only one system in LALINET, namely the system MAO, is fully automatic. The remaining LALINET systems (8 of 9 systems, around 88.9%) require attended operation, therefore are limited by manpower costs and, thus, generally have a reduced temporal coverage. LALINET is aware of this necessity and is currently moving to quality assured unattended instruments, which in turn will have a positive impact on the manpower devoted on data analysis using tested retrieval algorithms (both individual-station developed and network unified algorithms (Barbosa et al., 2014)).

Systems' transportability in a non-standardized network is a key characteristic to check the performance and reliability of the individual lidar systems, to detect instrumental problems (Matthais et al., 2004) and to define a reference system. The analyses performed here are also meant to help designing the LALINET intercomparison field campaigns, indicating the systems and channels to be intercompared. The large number of mobile systems (6 out of 9, i.e. 66.7%) in LALINET would allow indeed for an intercomparison field campaign with simultaneous and collocated measurements and the logistics to transport the heavy containers across international boarders is currently in development. However, the existence of three laboratory-fixed systems (namely CUC, MEC, and SPU) prevents an overall intercomparison campaign with all systems simultaneously performing measurements at the same place. Thus, the LALINET instrumental intercomparison campaigns will have to follow the design of other lidar networks (Wandinger et al., 2015), i.e., defining master systems and transferring the intercomparison results to those laboratory-fixed systems. In this sense, two main campaigns have been planned (see details in Section 3.7).

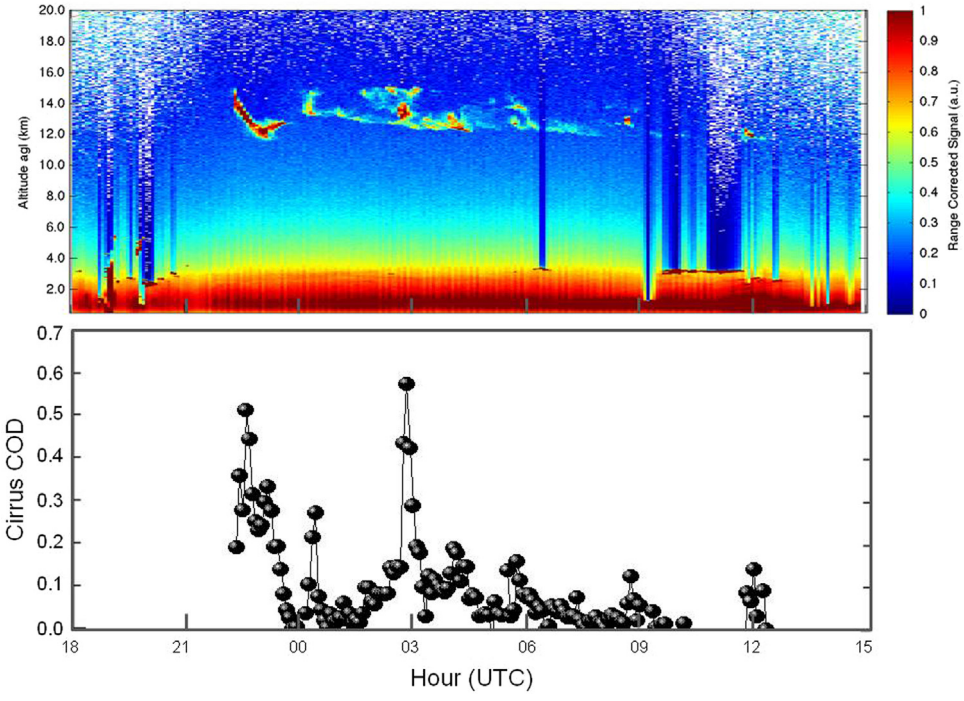

Fig. 2. Lidar data acquired at the LALINET MAO station from 18:00 UTC on 2nd June to 15:00 UTC on 3rd June 2014: (top) lidar range corrected signal at 355 nm, (bottom) cirrus cloud optical depth.

3.2. Emitter subsystem

Table 3 lists the main features related to the emitter subsystem. Other elements in a lidar system restricting the final derived atmospheric products are the multispectral capabilities of its laser source. A Nd:YAG laser, with a large variety of laser models, is currently the most frequent laser type in LALINET. The fundamental emission is at 1064 nm; nevertheless, the use of second and third harmonic generators also allows achieving emissions at 532 and 355 nm, respectively. LALINET has 8 instruments emitting laser pulses at 355 nm (88.9%), 8 at 532 nm (88.9%) and 7 at 1064 nm (77.8%). Hence, only 2 (22.2%) of the LALINET instruments do not fulfill the triad of wavelengths and, therefore, cannot provide a full set of Angström exponent or microphysical properties (see Section 3.4). The frequency repetition rates are variable from system to system, with the largest one in the systems CMR, MEC and NEU.

Regardless of the fact that lasers used in lidars are highly collimated, the use of beam expanders is an usual practice to reduce the background light in the probed atmospheric volume, to reduce the laser divergence and to reduce the probability of collecting multiple scattered light (Eloranta, 1998; Wandinger, 1998). In spite of the well-known benefits of using a beam expander, 9 emission channels in LALINET, all of them in the systems BAR, CMR and NEU, routinely operate without beam expander (39.9%). Overall, beam divergence for most of the channels in LALINET is larger than 0.4 mrad prior to applying expansion and less than 0.4 mrad in approximately 50% of the LALINET channels when expansion is applied.

3.3. Receiver subsystem

Table 4 lists the main features related to the receiver subsystem. Newtonian telescopes are frequently employed in LALINET (6 of 9 systems, i.e. 66.7%), in contrast to other lidar networks such as EARLINET (Pappalardo et al., 2014) where most of the lidar systems are Cassegrain-design based. Primary mirror sizes in LALINET range from 200 to 400 mm (in diameter) although they are usually below 250 mm (6 of 9 systems, i.e. 66.7%). However, owing to the presence of secondary mirrors, the obscuration area reduces telescope effective area. Secondary mirror sizes range from 47 to 90 mm (in diameter), being ≤ 70 mm in 6 of 9 systems (66.7%), which in turn cuts down the detection surface in 21–34%, depending on the system.

As a general rule, the lidar field-of-view (FOV) of the receiving telescope must be designed to keep a compromise between a small FOV necessary for high background suppression and a large FOV for an appropriate adjustment of the laser beam within the FOV and for enough signal intensity in the near range. Five instruments in LALINET have FOV below 1 mrad (55.6%), and consequently are unaffected by multiple scattering effects (Wandinger, 1998). In contrast, those instruments having larger FOVs, i.e. CUC, MAO, MEC and SPT, require multiple scattering corrections for investigating scenarios under high aerosol loads or cloudy atmospheres. The FOV-to-divergence ratio (ratio between FOV and laser beam divergence) is 1.8–3.2 in 6 LALINET systems. Systems such as the instruments LPZ and SPU are configured to have values as low as 0.2. However, an exception to these relatively low FOVs in the network is the instrument MEC, currently operation under a very large FOV of 19 mrad (i.e. FOV-to-divergence ratio of 38) because it is configured to study the lower troposphere, mostly inside the planetary boundary layer.

Another characteristic that makes LALINET different with respect to EARLINET is the predominance of coaxial configurations (6 systems, i.e. 66.7%), even though both coaxial and biaxial designs are used. Lidar performance in the near field mostly depends on the receiver configuration, affecting the overlap function. In order to perform quality assurance tests on LALINET systems, different internal checks have to be applied depending on the telescope.

3.4. Detection subsystem

Table 5 lists the main features related to the detection subsystem. Elastic channels in LALINET operate both at day- and nighttime. However, the number of instruments detecting at 1064 nm is low (3 systems, 33.3%), and not all systems measure signals at 355 (7 systems, 77.8%) and 532 nm (8 systems, 88.9%). The number of systems simultaneously detecting the triad of elastic lidar signals drastically diminishes up to 3 systems (33.3%), namely the instruments BAR, CMR and NEU. This fact constrains, to a certain degree, the multiwavelength capabilities of LALINET. As first consequence, the retrieval of Angström exponent profiles required for aerosol typing (Müller et al., 2007) is restrained. More dramatic is the consequence on particle microphysical retrievals. Most of the inversion codes to retrieve particle microphysical properties profiles from the synergetic combination of lidar and sun-photometry, namely LIRIC (Lidar-Radiometer Inversion Code) (Chaikovsky et al., 2015) and GARRLIC (Generalized Aerosol Retrieval From Radiometer and Lidar Combined) (Lopatin et al., 2013), demand for, at least, the triad of elastic lidar signals. Therefore, LALINET in its current status is not able to provide particle microphysical properties and, hence, is presently not able to contribute to improve the knowledge on the role of particle microphysics in the Earth's climate. The particle linear depolarization ratio is another key particle property for aerosol typing, for improving the LIRIC and GARRLIC microphysical retrievals. It is also the basis of POLIPHON (Polarizing Lidar Photometer Networking) (Tesche et al., 2009; Mamouri and Ansmann, 2014), as this algorithm retrieves the mass concentration of each component of an external mixture of two aerosol types with markedly different sphericities. Depolarization capabilities are missing in LALINET (apart from the instrument CMR in Argentina), whereby

Table 4
Some technical specifications regarding the receiver optics subsystem for the LALINET lidar stations.

Lidar system	Telescope type	Primary mirror diam. (mm)	Telescope obscuration diam. (mm)	Focal length (m)	Full field of view (mrad)	Telescope-laser axes distance (cm)
BAR	Cassegrain	203	69	2.0	0.9	0
CMR	Newtonian	203	56	1	1	0
CUC	Newtonian	400	85	1.8	1.6	0
LPZ	Newtonian	250	80	0.7	0.4	26
MAO	Cassegrain	400	90	4	1.75	32
MEC	Newtonian	200	47	1.2	19	0
NEU	Newtonian	203	56	1	1	0
SPT	Cassegrain	200	52	1	1.25	17
SPU	Newtonian	300	70	1.5	0.1	0

Table 5
Some technical specifications regarding the wavelength separation unit for the LALINET lidar stations. Day and/or night availability is included. Full width at half maximum is also given in brackets (in nm).

Lidar system	Elastic wavelengths (nm)			Raman wavelengths (nm)			
	355	532	1064	387	408	607	660
BAR	D/N (1)	D/N (1)	D/N (1)	–	–	–	–
CMR	D/N (1)	D/N[a] (1)	D/N (1)	–	–	–	–
CUC	D/N (1)	D/N (1)	–	N (0.25)	N (0.25)	–	–
LPZ	–	D/N (1)	–	–	–	–	–
MAO	D/N (1.12)	–	–	N (0.88)	N (0.97)	–	–
MEC	D/N (10)	D/N (2)	–	–	–	–	–
NEU	D/N (1)	D/N (1)	D/N (1)	–	–	–	–
SPT	–	D/N (0.5)	–	–	–	N (1)	–
SPU	D/N (1)	D/N (1)	–	D/N (0.25)	N (0.25)	D/N (0.25)	N (0.25)

[a] Detection of parallel and cross components.

the network plans to include depolarization capabilities in the operative instruments and also to spread into strategic areas where the impact of long-range transport of Saharan dust is feasible, such as the northernmost part of South America and the Caribbean Sea.

Despite the fact that Raman shifted channels traditionally operate at nighttime, some of the Raman channels in LALINET also operate during daytime. Nevertheless, the retrieval of particle optical properties from Raman signals is not as trustable as desirable yet. The network capability to derive independent profiles of particle extinction and backscatter (and hence particle lidar ratio) is limited due to the reduced number of N_2-Raman channels (3 systems at 387 and 2 systems at 607 nm), which in turn constrains the establishment of an aerosol typing in LALINET. Some studies point out that only the combination of independent particle extinction and backscatter coefficients can retrieve accurate microphysical properties (e.g. Veselovskii et al., 2002; Müller et al., 1999; Osterloh et al., 2013; Müller et al., 2015), and, consequently, those lidars providing three backscatters and two extinctions, namely 3+2 lidars, turn into an optimum election for particle microphysical characterization. Currently none of the LALINET instrument detect simultaneously Raman shifted signals at 387 and 607 nm and elastic signal at 1064 nm and, thus, the application of inversion with regularization cannot be accomplished.

Water vapor Raman channels are also routinely operated in LALINET and, hence, the retrieval of water vapor mixing ratio is achieved in several South American stations. This retrieval is based on the simultaneous measurement of a couple of Raman signals, one of them used as a reference (N_2-Raman shifted: 387 or 607 nm) and another is related to the gas under investigation (H_2O-Raman shifted: 408 or 660 nm). The relative high number of LALINET instruments simultaneously acquiring the couple of signals 387/408 nm (3 systems) and 607/660 nm (1 system) is valuable in South America. Beyond the retrieval of water vapor mixing ratio profiles, the water vapor capabilities of LALINET enables the research on hygroscopic growth of aerosol particles in this network (di Girolamo et al., 2012; Granados-Muñoz et al., 2015; Veselovskii et al., 2009).

3.5. Acquisition subsystem

Table 6 lists the main features related to the data acquisition subsystem. Lidar signal detection is attained with photomultipliers tubes (PMTs) and avalanche photodiodes (APDs), performing the detection in analog (AN) and photon-counting (PC) modes, preferred for near and far range, respectively. All LALINET instruments detect the elastic channels in AN mode but only 7 of 19 elastic channels also operate in PC mode (36.8%), constraining the signal detection range and reducing the far field signal-to-noise ratio. In turn, the entire lidar profile might be corrupted by the low signal-to-noise ratio in the far range since background correction is typically derived at high distances. Under situations of low signal-to-noise ratio in the far range, background has to be derived at relatively low heights, which in turn could contain aerosol traces. Thus, the measured signal could be underestimated. Therefore, simultaneous operation in AN and PC modes is desirable in all elastic channels of LALINET. Regarding Raman signals, they are typically measured in PC mode due to their intrinsic low intensity. However, owing to PMTs saturation in the near range, preventing the retrieval of trustable optical profiles, the instruments SPU and MAO detect Raman signals also in AN mode.

The 7.5-m spatial resolution is mostly standardized in LALINET (8 of 9 LALINET instruments, i.e. 88.9%); nevertheless, most of the instruments have selectable spatial resolutions (3.75, 7.5, 15 and 30 m). The maximum lidar-probed altitude is highly variable from a few kilometers (2 instruments, i.e. 22.2%) to more than one hundred kilometers (i.e. 5 of 9 instruments, 55.5%). The last one leads to the computation of background correction at high altitudes free from aerosol particles (both tropospheric and those stratospheric originated by volcanoes). Other systems, such as the instruments MAO and LPZ, count on a pretrigger device for signal acquisition before firing pulses, enabling the background subtraction using pretrigger data. However, only the system LPZ routinely operates it.

Table 6
Some technical specifications regarding acquisition subsystem for the LALINET lidar stations (AN: analog, PC: photon counting).

Lidar system	Detection mode							Vertical res. (m)	Max. Range (km agl)
	355	532	1064	387	408	607	660		
BAR	AN	AN	AN	–	–	–	–	7.5	122.8
CMR	AN	AN	AN	–	–	–	–	7.5	122.8
CUC	AN	AN	–	PC	PC	–	–	7.5	64
LPZ	–	AN	–	–	–	–	–	15	15
MAO	AN/PC	–	–	AN/PC	PC	–	–	7.5	122.8
MEC	AN/PC	AN/PC	–	–	–	–	–	7.5	12
NEU	AN	AN	AN	–	–	–	–	7.5	122.8
SPT	–	AN/PC	–	–	–	PC	–	7.5	120
SPU	AN/PC	AN/PC	AN/PC	AN/PC	AN/PC	AN/PC	AN/PC	7.5	30

3.6. Ancillary atmospheric instrumentation

Furthermore, additional instrumentation is available at each LALINET lidar station. In particular, Sun-photometric measurements are available in all the LALINET stations. CUC, MAO, MEC and Argentinean stations acquire Sun-photometer data co-located with the lidar systems, whereas Sun-photometers at LPZ, SPU and SPT stations are between 200 and 500 m far from the lidars systems. Such kind of short distances can be neglected for aerosol research on regional and continental scales; however, it is desirable the simultaneous and co-located performance of both instruments for local aerosol research and those synergic studies where temporal and spatial coincidence of lidar and Sun-photometer is required to derive trustable information (such as research involving LIRIC (Chaikovsky et al., 2015), GARRLIC (Lopatin et al., 2013) and POLIPHON (Tesche et al., 2009; Mamouri and Ansmann, 2014) algorithms to retrieve particle microphysical properties).

Radiosounding data give the thermodynamic characterization of the atmosphere and they are also used as input in the Klett and Raman methods to compute the molecular backscatter and molecular extinction profiles. However, only 4 LALINET stations (44.4%) (namely CMR, MAO, SPU and SPT) use nearby radiosoundings (distance between lidar and launching station less than 30 km). The MEC system counts with regular radiosoundings each 12 hours but a larger distance (200 km), and therefore, without reliable representativeness of the thermodynamic conditions above the lidar station. For those LALINET stations without radiosounding launches, it is recommendable the use of extended meteorological datasets provided by GDAS (Global Data Assimilation System, ftp://arlftp.arlhq.noaa.gov/pub/archives/gdas1), leading to generate interpolated meteorological data profiles over a grid of $1 \times 1^{\circ}$ each 3 h, therefore fulfilling the meteorological gap existing over many LALINET stations. Another option is use of the Weather Research and Forecasting (WRF) Model (http://www2.mmm.ucar.edu/wrf/users/). Based on terrestrial and satellite information, meteorological data can be retrieved for 1 km by 1 km grid with 35 vertical levels each 30 min.

3.7. Intercomparison field campaigns

The focus of the intercomparison field campaigns is (i) checking the continuous improvement of the instruments during the years; (ii) defining, qualifying and testing reference systems and (iii) potentially integrating new LALINET stations.

The first intercomparison campaign will be a joint initiative of LALINET, ESA (European Space Agency) and EARLINET. This campaign was conceived to sequentially compare, from the hardware point of view, an EARLINET reference system with the systems in Brazil and Argentina. Additionally, this campaign is expected to contribute to the validation of a new lidar system that is going to be installed at Natal (Northeastern coast of Brazil) that will start routine operation in 2016. This first campaign will be crucial for the performance of the whole network because it will qualify systems which can serve as LALINET traveling standards thereafter.

The second intecomparison campaign is going to take place at the Instituto de Pesquisas Energéticas e Nucleares (IPEN) where the system SPU is installed, intercomparing the systems BAR, CMR, MAO, NEU, LPZ, SPU and SPT (step 1). Because the mobile systems BAR, CMR and NEU are systems with the most complete capabilities, one of the Argentinean lidars (qualified during the first intercomparison campaign) may be deemed as master system. Afterwards, the master system has sequentially to move to the fixed stations CUC and MEC for further intercomparisons (steps 2 and 3, respectively). The intercomparison steps 2 and 3 might be more profitable for the network if the Argentinean reference system increases its Raman capabilities before the intercomparison campaigns. After the intercomparison campaigns, LALINET will be able to more robustly respond to relevant scientific issues such as the characterization of the patterns of long-range transport of aerosol particles over South America, including biomass burning, volcanic particles and Saharan mineral dust. In a greater perspective, a well calibrated and standardized LALINET will be vital to provide support to space agencies for validation purposes of the current and future space-borne active remote sensing missions such as CALIPSO, CATS, ADM-Aeolus, EarthCARE and ACE over an area of unique aerosol and cloud conditions.

All theses intercomparison campaigns are expected to reinforce the confidence in the LALINET systems and their data quality, and will offer actions to be done for improvements in some instruments and to identify major challenges that need to be tackled in the future.

3.8. General recommendations

After the analysis of instrumental configurations in LALINET, some general recommendations on different features are listed:

(i) To get quality assured unattended instruments in order to reduce the manpower devoted to perform measurements.
(ii) To increase the number of emitted wavelengths in order to achieve the triad $355+532+1064$ nm in all systems, allowing for studies on aerosol typing and vertically-resolved microphysical properties.
(iii) To achieve the so-called $3+2$ configuration, offering detection of backscatter coefficient at three wavelengths and extinction coefficient at two wavelengths. Such kind of systems offers multiple benefits: enhancement the optical characterization of aerosols via the derivation of the spectral dependence of different properties; derivation of particle microphysical properties using of inversion algorithms with regularization; and improvements on the characterization in the lowermost part of the troposphere, increasing the knowledge on the planetary boundary layer and, therefore, on air quality.
(iv) To implement multiple scattering corrections on specific instruments with large FOV when these stations undergo high-loading events, such as sugar cane burning episodes, or when performing cloud studies.
(v) To initiate depolarization measurements, which are almost missing over South America and constraining the LALINET capabilities to attend to relevant issues such as aerosol typing. Hugely advisable is the incorporation of depolarization channels in strategic areas where the impact of long-range transport of Saharan dust is feasible, such as the northernmost part of South America and the Caribbean Sea or regions where volcanic aerosols frequently affect the air quality such as Argentina and Chile, allowing for the discrimination among different aerosol types.

4. Conclusions

This article presented a study conceived to investigate the current instrumental configuration of LALINET with the aim of highlighting the instrumental strengths and weaknesses of this network. The low number of simultaneously measured wavelengths of the systems was revealed as the main drawback of the network, inhibiting a proper characterization of the aerosol field over South America. Besides, the almost non-existing depolarization capabilities along the network restrict even more an aerosol typing here. As a result, LALINET, in its current status, cannot provide all the vertical-resolved aerosol information that would be

desirable for a proper environmental and climate characterization. Interestingly, LALINET offers the opportunity of investigating hygroscopic growth-related issues that are a key to understand the climate system due to the relatively great coverage of systems with such capabilities and the unique atmospheric scenarios over the continent.

LALINET is a community avid of increasing its knowledge, where the exchange of expertise with international experts and other networks is its cornerstone. Lidar research over Latin America can benefit from the complementary use of other instrumental networks such using sun-photometers and other instruments for high-quality aerosol and meteorological research. LALINET is a living network under continuous development not only at instrumental and algorithmic level but also in terms of coverage. The results of the diagnosis on the LALINET instrumentation will benefit to both the existing stations and those to be installed in the future, and will help the improvement of the whole quality of the aerosol data products derived from this network for contributing, among others, to air quality studies, space agencies validation purposes and the scientific knowledge in general.

Acknowledgments

The authors acknowledge EARLINET (European Aerosol Research Lidar Network), AD-NET (Asian Dust Network) and ACTRIS-2 (Aerosols, Clouds, and Trace gases Research InfraStructure Network, Grant agreement no. 654109) for their support and exchange of expertise. This work was funded by FAPESP (Fundação da Amparo à Pesquisa do Estado de São Paulo) through the visiting professor Grant ref. 2013/21087-7 and projects 2011/14365-5 and 2008/58104-8; by the University of Granada through the contract “Plan Propio. Programa 9. Convocatoria 2013”; by the Spanish Ministry of Economy and Competitiveness through projects CGL2010-18782, CSD2007-00067, CGL2011-13580-E/CLI and CGL2011-16124-E; by the Andalusian Regional Government through projects P10-RNM-6299 and P12-RNM-2409; and by FONDECYT Project no. 11110126 for CUC station in Chile.

References

Ansmann, A., Wandinger, U., Riebesell, M., Weitkamp, C., Michaelis, W., 1992. Independent measurement of extinction and backscatter profiles in cirrus clouds by using a combined Raman elastic-backscatter lidar. Appl. Opt. 31, 7113–7131.

Antuña, J.C., Estevan, R., Barja, B., 2012. Demonstrating the potential for first-class research in underdeveloped countries: research on stratospheric aerosols and cirrus clouds optical properties, and radiative effects in Cuba (1988–2010). Bull. Am. Meteorol. Soc. 93, 1017–1027. http://dx.doi.org/10.1175/BAMS-d-11-00149.1.

Antuña-Marrero, J.C., Landulfo, E., Estevan, R., Barja, B., Robock, A., Wolfram, E., Ristori, P., Clemesha, B., Simonich, D., Zaratti, F., Forno, R., Armandillo, E., Bastidas, A.E., de Frutos-Baraja, A.M., Whiteman, D., Quel, E., Barbosa, H.M.J., Lopes, F., Montilla-Rosero, E., Guerrero-Rascado, J.L., submitted for publication. LALINET: the first Latin American-born regional atmospheric observational network. B. Am. Meteorol. Soc.

Baars, H., Ansmann, A., Althausen, D., Engelmann, R., Heese, B., Müller, D., Artaxo, P., Paixao, M., Pauliquevis, T., Souza, R., 2012. Aerosol profiling with lidar in the Amazon Basin during the wet and dry season. J. Geophys. Res. 117, D21201. http://dx.doi.org/10.1029/2012JD018338.

Barbosa, H.M.J., Barja, B., Pauliquevis, T., Gouveia, D.A., Artaxo, P., Cirino, G.G., Santos, R.M.N., Oliveira, A.B., 2014. A permanent raman lidar station in the Amazon: description, characterization and first results. Atmos. Meas. Tech. 7, 1745–1762. http://dx.doi.org/10.5194/amt-7-1745-2014.

Barbosa, H.M.J., Lopes, F.J.S., Silva, A., Nisperuza, D., Barja, B., Ristori, P., Gouveia, D. A., Jimenez, C., Montilla, E., Mariano, G.L., Landulfo, E., Bastidas, A., Quel, E.J., 2014. The first ALINE measurements and intercomparison exercise on lidar inversion algorithms. Ópt. Pura Apl. 47 (2), 99–108.

Boucher, O., Randall, D., Artaxo, P., Bretherton, C., Feingold, G., Forster, P., Kerminen, V.-M., Kondo, Y., Liao, H., Lohmann, U., Rasch, P., Satheesh, S.K., Sherwood, S., Stevens, B., Zhang., X.Y., 2013. Clouds and aerosols. In: Stocker, T.F., Qin, D., Plattner, G.-K., Tignor, M., Allen, S.K., Boschung, J., Nauels, A., Xia, Y., Bex, V., Midgley, P.M. (Eds.), Climate Change 2013: The Physical Science Basis. Contribution of Working Group I to the Fifth Assessment Report of the Intergovernmental Panel on Climate Change. Cambridge University Press, Cambridge, United Kingdom and New York, NY, USA.

Cairo, F., di Donfrancesco, G., Adriani, A., Pulvirenti, L., Fierli, F., 1999. Comparison of various linear depolarization parameters measured by lidar. Appl. Opt. 38, 4425–4432.

Chaikovsky, A., Dubovik, O., Holben, B., Bril, A., Goloub, P., Tanré, D., Pappalardo, G., Wandinger, U., Chaikovskaya, L., Denisov, S., Grudo, Y., Lopatin, A., Karol, Y., Lapyonok, T., Amiridis, V., Ansmann, A., Apituley, A., Alados-Arboledas, L., Binietoglou, I., Boselli, A., D'Amico, G., Freudenthaler, V., Giles, D., Granados-Muñoz, M.J., Kokkalis, P., Nicolae, D., Oshchepkov, S., Papayannis, A., Perrone, M. R., Pietruczuk, A., Rocadenbosch, F., Sicard, M., Slutsker, I., Talianu, C., De Tomasi, F., Tsekeri, A., Wagner, J., Wang, X., 2015. Lidar-Radiometer Inversion Code (LIRIC) for the retrieval of vertical aerosol properties from combined lidar/radiometer data: development and distribution in EARLINET. Atmos. Meas. Tech. Discuss. 8, 12759–12822. http://dx.doi.org/10.5194/amtd-8-12759-2015.

da Costa, R.F., Bourayou, R., Landulfo, E., Guardani, R., Veselovskii, I., Steffens, J., 2013. Stand-off mapping of the soot extinction coefficient in a refinery flare using a 3-wavelength elastic backscatter LIDAR. Proc. SPIE 8894, 1–6. http://dx.doi.org/10.1117/12.2027240 88940P.

da Costa, R.F., Steffens, J., Landulfo, E., Guardani, R., Nakaema, W.M., Moreira Jr, P.F., Lopes, F.J.S., Ferrini, P., 2011. Real-time mapping of an industrial flare using LIDAR. Proc. SPIE 8182, 1–7. http://dx.doi.org/10.1117/12.897907 81820Y.

Eloranta, E.W., 1998. Practical model for the calculation of multiply scattered lidar returns. Appl. Opt. 37, 2464–2472.

Fernald, F.G., 1984. Analysis of atmospheric lidar observations: some comments. Appl. Opt. 23, 652–653.

Fernald, F.G., Herman, B.M., Reagan, J.A., 1972. Determination of aerosol height distribution by lidar. J. Appl. Meteorol. 11, 482–489.

Freudenthaler, V., Esselborn, M., Wiegner, M., Heese, B., Tesche, M., Ansmann, A., Müller, D., Althausen, D., Wirth, M., Fix, A., Ehret, G., Knoppertz, P., Toledano, C., Gasteiger, J., Garhammer, M., Seefeldner, M., 2009. Depolarization ratio profiling at several wavelengths in pure Saharan dust during SAMUM 2006. Tellus Ser. B – Chem. Phys. Meteorol. 61, 165–179.

di Girolamo, P., Summa, D., Bhawar, R., di Iorio, T., Cacciani, M., Veselovskii, I., Dubovik, O., Kolgotin, A., 2012. Raman lidar observations of a Saharan dust outbreak event: characterization of the dust optical properties and determination of particle size and microphysical parameters. Atmos. Environ. 50, 66–78.

Gouveia, D.A., Barja, B., Barbosa, H.M.J., 2014. Characterization of cirrus clouds in central Amazon (2.89°S 59.97°W): firsts results from six months of observations in 2011. Ópt. Pura Apl. 47 (2), 109–144. http://dx.doi.org/10.7149/OPA.47.2.109.

Granados-Muñoz, M.J., Navas-Guzmán, F., Bravo-Aranda, J.A., Guerrero-Rascado, J.L., Valenzuela, A., Fernández-Gálvez, J., Lyamani, H., Titos, G., Alados-Arboledas, L., 2015. Hygroscopic growth of atmospheric aerosols based on active remote sensing and radiosounding measurements. Atmos. Meas. Tech. 8, 705–718. http://dx.doi.org/10.5194/amt-8-705-2015.

Guerrero-Rascado, J.L., da Costa, R.F., Bedoya, A.E., Guardani, R., Alados-Arboledas, L., Bastidas, A.E., Landulfo, E., 2014. Multispectral elastic scanning lidar for flares research: characterizing the electronic subsystem and application. Opt. Exp. 22 (25), 31063–31077.

Hartmann, D.L., Klein Tank, A.M.G., Rusticucci, M., Alexander, L.V., Brönnimann, S., Charabi, Y., Dentener, F.J., Dlugokencky, E.J., Easterling, D.R., Kaplan, A., Soden, B.J., Thorne, P.W., Wild, M., Zhai., P.M., 2013. Observations: atmosphere and surface. In: Stocker, T.F., Qin, D., Plattner, G.-K., Tignor, M., Allen, S.K., Boschung, J., Nauels, A., Xia, Y., Bex, V., Midgley, P.M. (Eds.), Climate Change 2013: The Physical Science Basis. Contribution of Working Group I to the Fifth Assessment Report of the Intergovernmental Panel on Climate Change. Cambridge University Press, Cambridge, United Kingdom and New York, NY, USA.

Holben, B.N., Eck, T.F., Slutsker, I., Tanré, D., Buis, J.P., Setzer, A., Vermote, E., Reagan, J.A., Kaufman, K.J., Nakajima, T., Lavenu, F., Jankowiak, I., Smirnov, A., 1998. Aeronet – a federated instrument network and data archieve for aerosol characterization. Rem. Sens. Environ. 66, 1–19.

Hu, Y., Liu, Z., Winker, D., Vaughan, M., Noel, V., Bissonnette, L., Roy, G., McGill, M., 2006. Simple relation between lidar multiple scattering and depolarization for water clouds. Opt. Lett. 31, 1809–1811. http://dx.doi.org/10.1364/OL.31.001809.

Klett, J.D., 1981. Stable analytic inversion solution for processing Lidar returns. Appl. Opt. 20, 211–220.

Klett, J.D., 1985. Lidar inversion with variable backscatter/extinction ratios. Appl. Opt. 24, 1638–1643.

Landulfo, E., Lopes, F.J.S., Mariano, G.L., Torres, A.S., de Jesus, W.C., Nakaema, W.M., Jorge, M.P.P., Mariani, R., 2010. Study of the properties of aerosols and the air quality index using a backscatter Lidar system and aeronet sunphotometer in the city of São Paulo, Brazil. J. Air Waste Manag. Assoc. 60, 386–392. http://dx.doi.org/10.3155/1047-3289.60.4.386.

Lopatin, A., Dubovik, O., Chaikovsky, A., Goloub, P., Lapyonok, T., Tanré, D., Litvinov, P., 2013. Enhancement of aerosol characterization using synergy of lidar and sun-photometer coincident observations: the GARRLiC algorithm. Atmos. Meas. Tech. 6, 2253–2325.

Machado, L.A.T., Silva Dias, M.A.F., Morales, C., Fisch, G., Vila, D., Albrecht, R., Goodman, S.J., Calheiros, A.J.P., Biscaro, T., Kummerow, C., Cohen, J., Fitzjarrald, D., Nascimento, E.L., Sakamoto, M.S., Cunningham, C., Chaboureau, J. –P., Petersen, W.A., Adams, D.K., Baldini, L., Angelis, C.F., Sapucci, L.F., Salio, P., Barbosa,

H.M.J., Landulfo, E., Souza, R.A.F., Blakeslee, R.J., Bailey, J., Freitas, S., Lima, W.F.A., Tokay, A., 2014. THE CHUVA PROJECT: how does convection vary across Brazil? Bull. Am. Meteor. Soc., 1365–1380 http://journals.ametsoc.org/doi/abs/10.1175/BAMS-d-13-00084.1.

Mamouri, R.E., Ansmann, A., 2014. Fine and coarse dust separation with polarization lidar. Atmos. Meas. Tech. Discuss. 7, 5173–5221.

Matthais, V., Freudenthaler, V., Amodeo, A., Balin, I., Balis, D., Bösenberg, J., Chaikovsky, A., Chourdakis, G., Comerón, A., Delaval, A., de Tomasi, F., Eixmann, R., Hågård, A., Komguem, L., Kreipl, S., Matthey, R., Rizi, V., Rodrigues, J.A., Wandinger, U., Wang, X., 2004. Aerosol lidar intercomparison in the framework of the EARLINET project. 1. Instruments. Appl. Opt. 43, 961–976.

Müller, D., Wandinger, U., Ansmann, A., 1999. Microphysical particle parameters from extinction and backscatter lidar data by inversion with regularization: theory. Appl. Opt. 38 (12), 2346–2357.

Müller, D., Ansmann, A., Mattis, I., Tesche, M., Wandinger, U., Althausen, D., Pisani, G., 2007. Aerosol-type-dependent lidar ratios observed with Raman lidar. J. Geophys. Res. Atmos. 112 (D16202), 1–11.

Müller, D., Böckmann, C., Kolgotin, A., Schneidenbach, L., Chemyakin, E., Rosemann, J., Znak, P., Romanov, A., 2015. Microphysical particle properties derived from inversion algorithms developed in the framework of EARLINET. Atmos. Meas. Tech. Discuss. 8, 12823–12885. http://dx.doi.org/10.5194/amtd-8-12823-2015.

Noel, V., Sassen, K., 2004.Study of ice crystal orientation in ice clouds based on polarized observations from the FARS scanning lidar. In: Reviewed and Revised Papers Presented at the 22nd International Laser Radar Conference (ILRC 2004), 12–16 July 2004, Matera, Italy. Edited Pappalardo, G., Amodeo, A., European Space Agency Spec. Publ., ESA SP-561, pp. 309–312.

Osterloh, L., Böckmann, C., Nicolae, D., Nemuc, A., 2013. Regularized inversion of microphysical atmospheric particle parameters: theory and application. J. Comp. Phys. 237, 79–94.

Pappalardo, G., Amodeo, A., Apituley, A., Comerón, A., Freudenthaler, V., Linné, H., Ansmann, A., Bösenberg, J., D'Amico, G., Mattis, I., Mona, L., Wandinger, U., Amiridis, V., Alados-Arboledas, L., Nicolae, D., Wiegner, M., 2014. EARLINET: towards an advanced sustainable European aerosol lidar network. Atmos. Meas. Tech. 7, 2389–2409.

Platt, C.M.R., 1978. Lidar backscatter from horizontal ice crystal plates. J. Appl. Meteorol. 17, 482–488.

Sassen, K., 1991. The polarization lidar technique for cloud research: a review and current assessment. Bull. Am. Meteorol. Soc. 72, 1848–1866.

Silva, A., Montilla-Rosero, E., Jiménez, C., Saavedra, C., Hernández, R., 2012. Tropospheric measurements of aerosol optical properties at Concepcion, Chile (36°S, 73°W). Reviewed and Revised Papers. In: 26th International Laser Radar Conference.

Takano, Y., Jayaweera, K., 1985. Scattering phase matrix for hexagonal ice crystals computed from ray optics. Appl. Opt. 24, 3254–3263.

Tesche, M., Ansmann, A., Müller, D., Althausen, D., Engelmann, R., Freudenthaler, V., Gross, S., 2009. Vertically resolved separation of dust and smoke over Cape Verde using multiwavelength Raman and polarization lidars during Saharan Mineral Dust Experiment 2008. J. Geophys. Res. 114, D13202. http://dx.doi.org/10.1029/2009JD011862.

Thomas, L., Cartwright, J.C., Wareing, D.P., 1990. Lidar observations of the horizontal orientation of ice crystals in cirrus clouds. Tellus, Ser. B 42, 211–216.

Veselovskii, I., Whiteman, D.N., Kolgotin, A., Andrews, E., Korenskii, M., 2009. Demonstration of aerosol property profiling by multiwavelength lidar under varying relative humidity conditions. J. Atmos. Ocean. Tech. 26 (8), 1543–1557.

Veselovskii, I., Kolgotin, A., Griaznov, V., Müller, D., Wandinger, U., Whiteman, D.N., 2002. Inversion with regularization for the retrieval of tropospheric aerosol parameters from multiwavelength lidar sounding. Appl. Opt. 41 (18), 3685–3699.

Wandinger, U., 1998. Multiple-scattering influence on extinction and backscatter-coefficient measurements with Raman and high-spectral-resolution lidars. Appl. Opt. 37, 417–427.

Wandinger, U., Freudenthaler, V., Baars, H., Amodeo, A., Engelmann, R., Mattis, I., Groß, S., Pappalardo, G., Giunta, A., D'Amico, G., Chaikovsky, A., Osipenko, F., Slesar, A., Nicolae, D., Belegante, L., Talianu, C., Serikov, I., Linné, H., Jansen, F., Apituley, A., Wilson, K.M., de Graaf, M., Trickl, T., Giehl, H., Adam, M., Comerón, A., Muñoz, C., Rocadenbosch, F., Sicard, M., Tomás, S., Lange, D., Kumar, D., Pujadas, M., Molero, F., Fernández, A.J., Alados-Arboledas, L., Bravo-Aranda, J.A., Navas-Guzmán, F., Guerrero-Rascado, J.L., Granados-Muñoz, M.J., Preißler, J., Wagner, F., Gausa, M., Grigorov, I., Stoyanov, D., Iarlori, M., Rizi, V., Spinelli, N., Boselli, A., Wang, X., Lo Feudo, T., Perrone, M.R., De Tomasi, F., Burlizzi, P., 2015. EARLINET instrument intercomparison campaigns: overview on strategy and results. Atmos. Meas. Tech. Discuss. 8, 10473–10522.

Wang, K., Dickinson, R.E., Liang, S., 2009. Clear sky visibility has decreased over land globally from 1973 to 2007. Science 323, 1468–1470.